Atom-Chip Fountain Gravimeter

S. Abend,[1,*] M. Gebbe,[2] M. Gersemann,[1] H. Ahlers,[1] H. Müntinga,[2] E. Giese,[3,4] N. Gaaloul,[1]
C. Schubert,[1] C. Lämmerzahl,[2] W. Ertmer,[1] W. P. Schleich,[3,5] and E. M. Rasel[1]

[1]*Institut für Quantenoptik, Leibniz Universität Hannover, Welfengarten 1, D-30167 Hannover, Germany*
[2]*ZARM, Universität Bremen, Am Fallturm, D-28359 Bremen, Germany*
[3]*Institut für Quantenphysik and Center for Integrated Quantum Science and Technology (IQST),
Universität Ulm, Albert-Einstein-Allee 11, D-89081 Ulm, Germany*
[4]*Department of Physics and Max Planck Centre for Extreme and Quantum Photonics,
University of Ottawa, 25 Templeton Street, Ottawa, ON K1N 6N5, Canada*
[5]*Texas A&M University Institute for Advanced Study (TIAS), Institute for Quantum Science and Engineering (IQSE)
and Department of Physics and Astronomy, Texas A&M University, College Station, Texas 77843-4242, USA*
(Received 13 May 2016; revised manuscript received 30 August 2016; published 11 November 2016)

We demonstrate a quantum gravimeter by combining the advantages of an atom chip for the generation, delta-kick collimation, and coherent manipulation of freely falling Bose-Einstein condensates (BECs) with an innovative launch mechanism based on Bloch oscillations and double Bragg diffraction. Our high-contrast BEC interferometer realizes tens of milliseconds of free fall in a volume as little as a one centimeter cube and paves the way for measurements with sub-μGal accuracies in miniaturized, robust devices.

Interferometers based on laser cooled atoms can measure inertial forces with high accuracy [1–6] and are now commercially available as gravimeters with an accuracy better than one part in 10^8 of gravity [7–9], which corresponds to 10 μGal (1 μGal $= 10^{-8}$ m/s^2). Bose-Einstein condensates (BECs) promise to improve these achievements and to reach [10,11] accuracies below a μGal. Atom chips have already been employed very successfully in cold atom experiments [12–14], in particular for guided [15] or trapped [16] matter wave interferometry, microwave clocks [17,18] and magnetometry [15,19]. In this Letter we demonstrate an atom-chip fountain gravimeter using BECs.

Our approach summarized in Fig. 1(a) offers several advantages with respect to present BEC gravimeters [20]: (i) It relies on the simple, robust, rapid, and efficient creation of BECs on atom chips and represents a promising way to portable BEC sensors. (ii) The atom chip facilitates all required atom-optical operations including Bragg interferometry and allows us to perform them in a volume of less than a one centimeter cube. (iii) Relaunching the atoms extends the time for state preparation and interferometry, which are both necessary ingredients for reaching a better accuracy in compact volumes.

We employ the atom chip for the complete state preparation, i.e. generation and release of BECs, delta-kick collimation featuring ultralow expansion rates [21,22], coherent transfer of atoms to the nonmagnetic state via adiabatic rapid passage, and Stern-Gerlach-type deflection of magnetic states. Furthermore, the atom chip serves as a retroreflector forming pulsed lattices which drive Bragg diffraction, Bloch oscillations [23–27], and combinations of both. These processes are crucial for launching as well as

coherently splitting, deflecting, and recombining a BEC to realize a Mach-Zehnder interferometer (MZI) [28].

In a MZI the phase shift $\phi = k_{\text{eff}} g T^2$ due to the gravitational acceleration g scales with the square of the free evolution time T between two Bragg processes and linearly with the atomic momentum $\hbar k_{\text{eff}} = 2n\hbar k$ transferred by the beam splitter, which depends on Planck's constant $\hbar$, the lattice wave vector $k = 2\pi/\lambda$ as well as the order n of the Bragg process. Hence, the sensitivity of the interferometer considerably benefits from an extension of T. However, in a compact device a BEC, when released, can only fall a short distance and, hence, T is limited as depicted in Fig. 1(b). Moreover, delta-kick collimation consumes a significant portion of the time of free fall.

In order to increase T and perform delta-kick collimation, we have developed an efficient and versatile launch mechanism based on the coherent momentum transfer by Bloch oscillations combined with double Bragg diffraction [29–31], which precedes the interferometry sequence as shown in Fig. 1(c). In this way, we extend T to several tens of milliseconds as obtained in larger devices [1,4,6], without increasing the complexity of the optical setup for the lattice. This extension represents an important step towards reaching accuracies below the μGal range.

Our gravimeter is implemented in the atom-chip apparatus reported in Ref. [32], which reliably produces BECs of ^{87}Rb within 15 s of up to 1.5×10^4 atoms in the hyperfine state $F = 2$, $m_F = 2$ and a shallow magnetic trap (46,31,18 Hz) at 50 nK. The atom chip allows us to perform delta-kick collimation which exploits the point-source character of the BEC. During the free fall of a BEC its mean-field energy gives rise to an accelerated expansion and the associated larger spatial distribution reflects
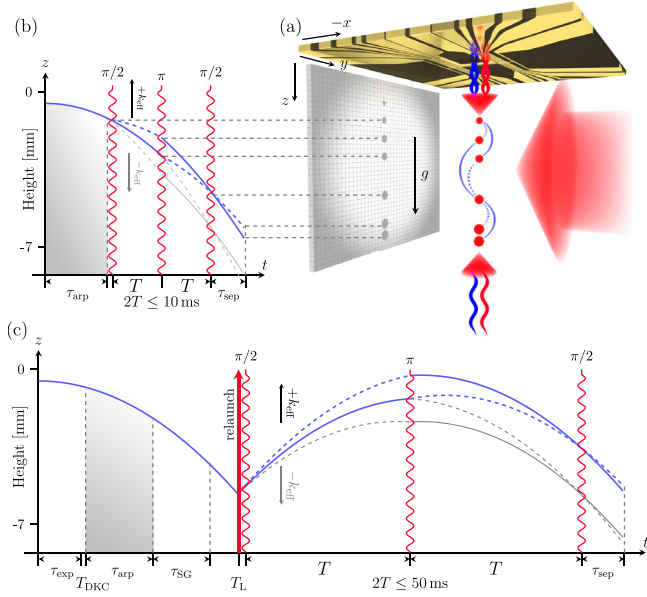
FIG. 1.   Atom-chip based gravimeter setup (a) and space-time trajectories (blue or gray dashed, solid lines) of a BEC without (b) and with (c) relaunch. The chip serves in all steps of state preparation and as retroreflector for light propagating in the z direction (red, blue wavy arrows), thus creating moving lattices, which induce Bragg diffraction or Bloch oscillations for interferometry with BECs (red dots). The number of atoms at the output port is obtained by imaging the spatial absorption (gray dots) of a light pulse traveling along the x direction with a CCD camera. Both space-time diagrams (b) and (c) start with the release of the BEC, and consist of (i) the adiabatic rapid passage to the Zeeman state with the lowest magnetic susceptibility during $\tau_{\mathrm{arp}} = 10.2$ ms, (ii) the MZI of variable duration $2T$, and (iii) the detection of the wave packets at the output ports, after they have moved apart for $\tau_{\mathrm{sep}} = 13$ ms at ToF $= 34$ and 97.6 ms. The MZI is formed by coherently splitting, redirecting, and recombining BECs by Bragg diffraction either in the upward (blue lines) or downward direction (gray lines). Unfortunately, the preparation takes up a considerable fraction of the free-fall time in scenario (b). In contrast, the coherent relaunch of (c) implemented by Bloch oscillations and double Bragg diffraction preceding the MZI allows us to incorporate delta-kick collimation at $\tau_{\mathrm{exp}} = 6$ ms after release to reduce the effect of the atomic interaction, as well as Stern-Gerlach-type deflection for $\tau_{\mathrm{SG}} = 7$ ms, and increases the sensitivity of the interferometer by up to 2 orders of magnitude.

directly the increased atomic velocity. However, a position-dependent force generated by a harmonic trap and applied for an appropriate time slows down the atoms. For this purpose, we employ the Ioffe-Pritchard trap (131,127,18 Hz) provided by the atom chip by quickly turning it on for $\tau_{\mathrm{dkc}} = 280$ μs after the BEC has expanded for $\tau_{\mathrm{exp}} = 6$ ms. In this way we reach effective temperatures of a few nK [21]. State preparation for interferometry ends with an adiabatic rapid passage to the Zeeman state $F = 2$, $m_F = 0$ induced by a chirped radio frequency pulse of duration $\tau_{\mathrm{arp}} = 10.2$ ms and pushing away residual

atoms in magnetic sensitive states by Stern-Gerlach-type deflection.

For the operation as a gravimeter, we have included in our device a vertical, linearly polarized light beam featuring a constant and a variable frequency component ν and $\nu + \Delta\nu(t)$, retroreflected by the atom chip [33]. In this way two counterpropagating accelerated lattices form and drive Bragg diffraction or Bloch oscillations. The beam aligned parallel to gravity to better than 10 mrad is generated by a frequency-doubled fiber-laser system (NKT Photonics, Koheras Boostik E15 with a Toptica Photonics SHG pro), that is 100 GHz blue-detuned from the $D2$ transition at 780.241 nm to suppress spontaneous emission. The two frequency components are generated by a single acousto-optical modulator (AA Opto Electronics, MT80-1.5-IR), that also adjusts the light power in the lattice. Up to 1 W of laser power is guided via a single-mode fiber to the experiment and collimated by a commercial fiber collimator (SuK, 60FC-4-A18) with a diameter of 3.3 mm to achieve the necessary lattice depths and Rabi frequencies. Gaussian-shaped pulses of a temporal width of $\tau_{\sigma} = 12$ to 25 μs were employed for driving Bragg diffraction serving either as beam splitter or reflector with 95% efficiency.

Figure 1 shows the space-time diagrams of a BEC after release in our chip-based gravimeter without (b) and with (c) a coherent relaunch in the z direction. After state preparation we form the MZI by first- or higher-order Bragg diffraction off one of the two moving lattices, and the lattice moving in opposite direction is Doppler-detuned due to our retroreflective setup. Indeed, we create a sequence of Bragg pulses which coherently split, redirect, and recombine the BEC. The frequency difference of the lasers can be adjusted such that there is either a momentum transfer in the up- or downward direction [10,34], which allows us to suppress the effect of recoil-dependent shifts on the interferometer phase with alternating momentum transfer [35,36]. The atom number at the output ports of the interferometer is detected below the atom chip by absorption imaging with a CCD camera. For this purpose a single circularly polarized light pulse of duration 100 μs and diameter 21 mm irradiates the atoms from the x direction and excites them to the $F = 3$ state. Detection without and with relaunch is performed at the lowest part of the detection volume at ToF $= 34$ and 97.6 ms, respectively. This arrangement includes sufficient time $\tau_{\mathrm{sep}} \approx 13$ ms for the separation of the wave packet to become detectable by our imaging system.

The free-fall rate of the BECs is measured by chirping the difference $\Delta\nu(t) = \alpha t + 2n\nu_{\mathrm{rec}}$ of the laser frequencies, starting from the recoil frequency $2n\nu_{\mathrm{rec}}$ with a rate α, such that the lattice motion precisely matches the acceleration of the atoms. Figure 2 shows the signal of our MZI without relaunch as a function of α for $T = 1$, 3, and 5 ms together with the Allan standard deviation [37] representing the increase in precision resulting from the measurement. For
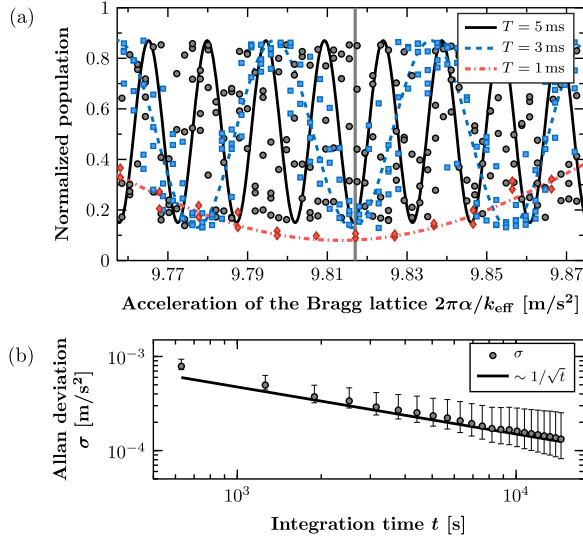
FIG. 2. Gravitational acceleration deduced from three signals without relaunch (a) and its Allan deviation (b). Dependence (a) of normalized atom numbers (red diamond, blue squares, black circles) in one output port of the MZI and corresponding sinusoidal fits (red dotted, blue dashed, and black solid lines) for $T = 1, 3, 5$ ms on the acceleration $2\pi\alpha/k_{\text{eff}}$ of the Bragg lattice. The interference signals reveal a high contrast of $C = 0.75$ thanks to the use of BECs and an increase of noise when T is extended due to higher intrinsic sensitivity. When the lattice acceleration is identical to the local gravitational acceleration, the interference signals assume the same minimum for all T (gray line). Allan deviation (b) of the acceleration (gray circles) and precision of our demonstrator improves with the square root (black line) of the integration time t during 8 h with $T = 5$ ms.

$T = 5$ ms the intrinsic relative sensitivity given per cycle reaches $\Delta g/g = 3.7 \times 10^{-6}$, which is only a factor of 1.5 above shot noise. The observed contrast $C = A/P_0 = 0.75$ given by the amplitude A of the sinusoidal signal divided by its mean P_0 is mainly caused by the imperfect adiabatic rapid passage due to limited radio frequency power.

Even when we include the first-order correction [38,39] for the nonvanishing pulse duration τ assuming box-shaped pulses, the total phase shift [40] $\phi_{\text{tot}} = (k_{\text{eff}}g - 2\pi\alpha)(T^2 + 3T\tau)$ vanishes independently of T and τ for the special case of $\alpha = k_{\text{eff}}g/(2\pi)$, where the atom number in one output port of the MZI assumes a minimum [1]. The inferred value of g agrees with the German gravity network [41]. The Allan standard deviation shown in Fig. 2(b) obtained by repeating the measurements with the maximal duration of $T = 5$ ms over 8 h yields a relative precision of $\Delta g/g = 1.3 \times 10^{-5}$. Since our experiment is operated in a rough environment without access to any vibrational shielding, the observed short-term stability is governed by the environmental vibrational noise, which was independently determined by an inertial measurement unit (iMU-FCR-E-03) to about 1.3×10^{-2} $(\text{m/s}^2)/\sqrt{\text{Hz}}$.

In order to enhance the sensitivity of our MZI and perform delta-kick collimation in the compact volume, we have developed a simple but effective method to coherently relaunch the atoms. Here we rely on the efficient transfer of a large number of photons, which exceeds other approaches [42,43] and so far has been demonstrated for successive Raman [44,45] or Bragg diffraction [46–48], Bloch oscillations [26,27], and by combinations of these [49–51]. Relaunching mechanisms relying on Bloch oscillations were either based on two crossed beams reflected on a mirror surface [52] or opposing laser beams [53]. Our approach considerably simplifies these schemes and relies on a single laser beam featuring two frequency components retroreflected from the surface of the atom chip.

Figure 3(a) shows the intensity (top) and velocity (bottom) of the lattice which drives Bloch oscillations, double Bragg diffraction and combinations of both as a function of time. The velocity is given in units of the photon recoil velocity $\hbar k/m$, where $\hbar k$ and m are momentum of a photon and atomic mass, respectively. Rather than accelerating BECs solely with Bloch oscillations (red dotted lines), our scheme is based on a three-step sequence (black solid lines): (i) A BEC is loaded into a downward-moving lattice by increasing the lattice depth to 15 recoil energies within 100 μs and is decelerated with an efficiency of 0.9995 per transferred recoil $\hbar k$ from velocities between -35 to $-50\hbar k/m$, down to $-8\hbar k/m$. At this velocity the deceleration is stopped and the BEC is adiabatically released from the lattice by linearly decreasing the power of the lattice beams within 100 μs. (ii) A few 100 μs later, a $16\hbar k$-double Bragg pulse [29–31] inverts the velocity to $+8\hbar k/m$ with up to 80% efficiency. (iii) Finally, the BEC is adiabatically transferred into an upward-moving lattice and accelerated to the final launch velocity to realize the fountain-like interferometer shown in Fig. 1(c).

Figure 3(b) contrasts absorption images of BECs accelerated either solely by Bloch oscillations (left and middle), or by our new scheme (right): Atoms can be decelerated almost without any loss by Bloch oscillations to a speed as low as $8\hbar k/m$ (left). However, the use of a retroreflector creates two lattices instead of one and large losses occur as atoms close to rest populate other bands, as shown for the case, where a BEC is accelerated from -8 to $+8\hbar k/m$ (middle). This problem can be reduced by combining Bloch oscillations with double Bragg diffraction (right), creating a technique which enjoys an efficiency of $> 75\%$, mainly limited due to the nonvanishing velocity spread of the expanding BEC.

Based on this method we have implemented a MZI with $T = 25$ ms and first-order Bragg diffraction without increasing the free-fall baseline of the experiment. Figure 3(c) shows the corresponding data for ToF $= 97.6$ ms. At this level of sensitivity vibrations induce the phase to scatter over the complete 2π interval and the determination of the interferometric contrast must
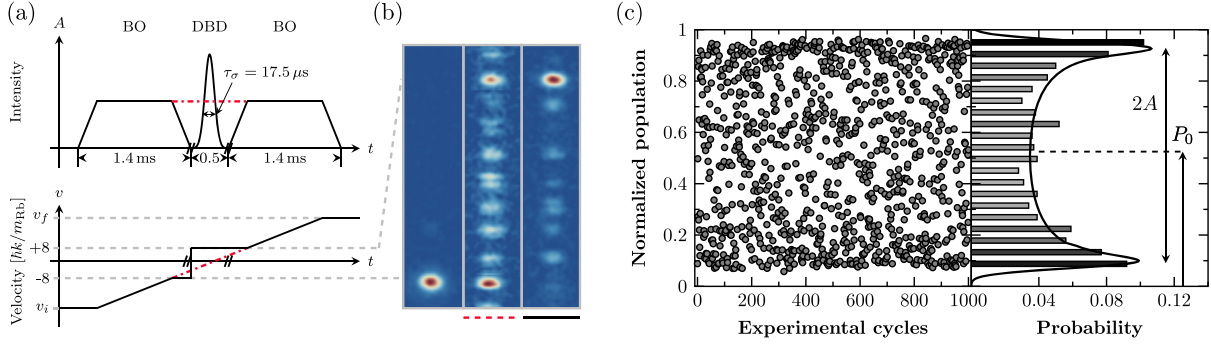
FIG. 3.   Atom-chip fountain gravimeter. Temporal dependence (a) of intensity (top) and velocity (bottom) of the optical lattice employed for relaunch. Absorption images (b) of BECs being accelerated either by Bloch oscillations (left, middle) or launched via a sequence composed of Bloch oscillations and double Bragg diffraction (right). Normalized populations in one output port of the MZI with relaunch and corresponding probability distribution of the signal (c). In both scenarios Bloch oscillations are implemented by adiabatically loading a freely falling BEC into and releasing it from an accelerated lattice by linearly changing the intensity (a). In the first case the lattice is uniformly accelerated from initial to final speed v_i and v_f by Bloch oscillations (red dotted lines), keeping lattice intensity and velocity chirp constant. In contrast, the optimal launch sequence consists of three steps: After deceleration by Bloch oscillations to $-8\hbar k/m$, a Gaussian-shaped light pulse drives double Bragg diffraction such that the BEC obtains $+8\hbar k/m$ followed by a second acceleration with Bloch oscillations (black solid lines). (b) Absorption images depict the corresponding atom distributions approximately 10 ms after the acceleration phases. Atoms can be decelerated almost lossless by Bloch oscillations to $-8\hbar k/m$ (left). However, large losses occur when the speed temporarily vanishes as in the case of an acceleration from -8 to $+8\hbar k/m$ (middle). The launch efficiency is enhanced to 75% by our new method (right). (c) With relaunch, the MZI can be extended to larger times leading to an improved sensitivity. The normalized interference signal obtained for $T = 25$ ms with first-order Bragg diffraction, reveals that vibrations induce the phase to scatter over the complete 2π interval. Nevertheless, the contrast determined by statistical analysis of the signal fluctuations [54] is $C = A/P_0 = 0.8$, corresponding to a 20-fold increased intrinsic sensitivity of $\Delta g/g = 1.7 \times 10^{-7}$.

be performed with the help of a statistical analysis [47,54–56] of the interferometer signal. The histogram of the relative population distribution reveals a contrast of about $C = 0.8$, which, due to the improved atomic preparation, is even larger than $C = 0.75$ in the previous case and corresponds to a 20-fold increased intrinsic sensitivity of $\Delta g/g = 1.7 \times 10^{-7}$, a level similar to Ref. [53].

Our relaunch method allows us to extend the time of free fall up to ToF = 135 ms in the given volume. Since state preparation and final separation consume $\tau_{\text{prep}} = 45$ ms and $\tau_{\text{sep}} = 15$ ms, respectively, the free-fall time can be pushed to at least $T = 35$ ms. With an advanced chip design [57] featuring an atomic flux of 10^5 launched atoms/ s in combination with fourth-order Bragg diffraction, for which we have obtained beam splitter efficiencies of 90%

leading to a contrast of $C = 0.7$, an intrinsic sensitivity of $(\Delta g/g)/\sqrt{\text{Hz}} = 5.3 \times 10^{-9}$ seems feasible.

The main drive for BEC sensors is a gain in accuracy. Indeed, BECs in combination with delta-kick collimation allow us to reduce the influence of important systematic uncertainties achieving fractions of a μGal. Table I lists the causes suspected to provide the largest contributions to the measurement uncertainty in a future, vibration-insensitive device as well as corresponding mitigation strategies.

For example, by first lowering the atomic density via the spreading of the wave packet and stopping this process by delta-kick collimation [21,22], phase shifts introduced by the mean field [20] can be sufficiently suppressed while expansion rates corresponding to nK temperatures are achievable. Moreover, the fluctuations of the launch

TABLE I.   Signal-to-noise ratio and leading systematic uncertainties measuring local gravity below $\Delta g/g < 1 \times 10^{-9}$ in less than 100 s of integration. We assume a gravimeter with $T = 35$ ms, coherent relaunch, fourth-order Bragg diffraction, and a free-fall baseline that does not exceed 1 cm.

Effect	Mitigation strategy	Noise $(\Delta g/g)/\sqrt{\text{Hz}}$	Bias $\Delta g/g$
Intrinsic sensitivity limit	Next generation source with 10^5 launched atoms/s [57]	5.3×10^{-9}	0
Mean field shift	Controlled expansion and delta-kick collimation [20,21]	1.5×10^{-10}	6.4×10^{-11}
Initial launch velocity	Scatter 120 μm/s, bias perpendicular to gravity below 30 μm/s [10]	1.5×10^{-12}	3.1×10^{-13}
Wave front quality	$\lambda/10$ chip-coating $\varnothing = 3$ cm and beam $\varnothing = 2$ cm [58,59]	6.7×10^{-10}	2.8×10^{-10}
Self gravity of atom chip	Appropriately designed mass distribution and modeling [60]	1.2×10^{-12}	5×10^{-10}
Targeted gravity estimation	Uncertainty after 100 s of integration		$\approx 7.8 \times 10^{-10}$

velocity [10], which cause a bias due to the Coriolis effect, can be characterized to the required level and optimized by the release procedure tested in our apparatus. Phase shifts resulting from the wave front curvature are insignificant since BECs are smaller and expand slower compared to thermal clouds [58,59]. We also emphasize that with the point-source nature [21,61] of BECs we can characterize systematic errors arising from wave-front distortions [58,59].

The surface quality of the chip is crucial for higher-order double Bragg diffraction and Bloch oscillations in order to preserve the high efficiencies and contrasts obtained for lower orders. Atom chips with the required optical surfaces of interferometric qualities were reported in Refs. [62–64]. The proximity of atoms close to the chip also leads to a phase shift and hence a measurement bias due to its gravity [60]. Fortunately, a mass reduction of the chip mount by two is sufficient to reach the targeted level. Moreover, a finite-element analysis of the mass distribution of the chip mount allows us to calculate the self-gravity effect at least with an accuracy at the 10% level.

Finally, it is remarkable that, compared to Raman diffraction, the influence of light shifts is reduced in interferometers based on Bragg diffraction. Indeed, these effects scale [65] with the third power of the inverse of the atomic velocity and are thus negligible for our relaunch parameters.

In conclusion, we have demonstrated the first atom-chip gravimeter employing BEC interferometry without and with relaunch. For the latter, we have realized a new scheme leading to an extended interferometer time in a compact volume of only a one centimeter cube. We claim an intrinsic sensitivity of a few μGal$/\sqrt{\text{Hz}}$ and sub-μGal accuracies in an optimized setup.

Further miniaturization should be possible by performing chip-assisted state preparation and relaunching with a pyramidal-shaped retroreflector [7]. Additionally, intracavity interferometry [66] may reduce the laser power required to drive Bloch oscillations, and hence, simplify the setup. However, already today our atom-chip gravimeter opens a new pathway to compact backpack-sized devices for high-precision absolute gravimetry in geodetic Earth observation and exploration.

[*]To whom correspondence should be addressed.
abend@iqo.uni-hannover.de

[1] A. Peters, K. Y. Chung, and S. Chu, Measurement of gravitational acceleration by dropping atoms, Nature (London) **400**, 849 (1999).

[2] A. Gauguet, T. Mehlstäubler, T. Lévèque, J. Le Gouët, W. Chaibi, B. Canuel, A. Clairon, F. Pereira Dos Santos, and A. Landragin, Off-resonant Raman transition impact in an atom interferometer, Phys. Rev. A **78**, 043615 (2008).

[3] J. K. Stockton, K. Takase, and M. A. Kasevich, Absolute Geodetic Rotation Measurement Using Atom Interferometry, Phys. Rev. Lett. **107**, 133001 (2011).

[4] Z.-K. Hu, B.-L. Sun, X.-C. Duan, M.-K. Zhou, L.-L. Chen, S. Zhan, Q.-Z. Zhang, and J. Luo, Demonstration of an ultrahigh-sensitivity atom-interferometry absolute gravimeter, Phys. Rev. A **88**, 043610 (2013).

[5] P. Berg, S. Abend, G. Tackmann, C. Schubert, E. Giese, W. P. Schleich, F. A. Narducci, W. Ertmer, and E. M. Rasel, Composite-Light-Pulse Technique for High-Precision Atom Interferometry, Phys. Rev. Lett. **114**, 063002 (2015).

[6] C. Freier, M. Hauth, V. Schkolnik, B. Leykauf, M. Schilling, H. Wziontek, H.-G. Scherneck, J. Müller, and A. Peters, Mobile quantum gravity sensor with unprecedented stability, arXiv:1512.05660.

[7] Q. Bodart, S. Merlet, N. Malossi, F. Pereira Dos Santos, P. Bouyer, and A. Landragin, A cold atom pyramidal gravimeter with a single laser beam, Appl. Phys. Lett. **96**, 134101 (2010).

[8] Muquans, http://www.muquans.com/.

[9] AOSense, http://www.aosense.com/.

[10] A. Louchet-Chauvet, T. Farah, Q. Bodart, A. Clairon, A. Landragin, S. Merlet, and F. Pereira Dos Santos, The influence of transverse motion within an atomic gravimeter, New J. Phys. **13**, 065025 (2011).

[11] D. Aguilera et al., STE-QUEST—test of the universality of free fall using cold atom interferometry, Classical Quantum Gravity **31**, 115010 (2014).

[12] W. Hänsel, P. Hommelhoff, T. W. Hänsch, and J. Reichel, Bose–Einstein condensation on a microelectronic chip, Nature (London) **413**, 498 (2001).

[13] R. Folman, P. Krüger, J. Schmiedmayer, J. Denschlag, and C. Henkel, Microscopic atom optics: From wires to an atom chip, Adv. At. Mol. Opt. Phys. **48**, 263 (2002).

[14] J. Fortágh and C. Zimmermann, Magnetic microtraps for ultracold atoms, Rev. Mod. Phys. **79**, 235 (2007).

[15] R. Bücker, J. Grond, S. Manz, T. Berrada, T. Betz, C. Koller, U. Hohenester, T. Schumm, A. Perrin, and J. Schmiedmayer, Twin-atom beams, Nat. Phys. **7**, 608 (2011).

[16] G.-B. Jo, Y. Shin, S. Will, T. A. Pasquini, M. Saba, W. Ketterle, D. Pritchard, M. Vengalattore, and M. Prentiss, Long Phase Coherence Time and Number Squeezing of Two Bose–Einstein Condensates on an Atom Chip, Phys. Rev. Lett. **98**, 030407 (2007).

[17] M. F. Riedel, P. Böhi, Y. Li, T. W. Hänsch, A. Sinatra, and P. Treutlein, Atom-chip-based generation of entanglement for quantum metrology, Nature (London) **464**, 1170 (2010).

[18] R. Szmuk, V. Dugrain, W. Maineult, J. Reichel, and P. Rosenbusch, Stability of a trapped-atom clock on a chip, Phys. Rev. A **92**, 012106 (2015).

[19] T. Berrada, S. van Frank, R. Bücker, T. Schumm, J.-F. Schaff, and J. Schmiedmayer, Integrated Mach–Zehnder interferometer for Bose–Einstein condensates, Nat. Commun. **4** (2013).

[20] J. E. Debs, P. A. Altin, T. H. Barter, D. Döring, G. R. Dennis, G. McDonald, R. P. Anderson, J. D. Close, and N. P. Robins, Cold-atom gravimetry with a Bose–Einstein condensate, Phys. Rev. A **84**, 033610 (2011).

[21] H. Müntinga et al., Interferometry with Bose–Einstein Condensates in Microgravity, Phys. Rev. Lett. **110**, 093602 (2013).

[22] T. Kovachy, J. M. Hogan, A. Sugarbaker, S. M. Dickerson, C. A. Donnelly, C. Overstreet, and M. A. Kasevich, Matter Wave Lensing to Picokelvin Temperatures, Phys. Rev. Lett. **114**, 143004 (2015).

[23] M. Ben Dahan, E. Peik, J. Reichel, Y. Castin, and C. Salomon, Bloch Oscillations of Atoms in an Optical Potential, Phys. Rev. Lett. **76**, 4508 (1996).

[24] S. R. Wilkinson, C. F. Bharucha, K. W. Madison, Q. Niu, and M. G. Raizen, Observation of Atomic Wannier-Stark Ladders in an Accelerating Optical Potential, Phys. Rev. Lett. **76**, 4512 (1996).

[25] E. Peik, M. Ben Dahan, I. Bouchoule, Y. Castin, and C. Salomon, Bloch oscillations of atoms, adiabatic rapid passage, and monokinetic atomic beams, Phys. Rev. A **55**, 2989 (1997).

[26] P. Cladé, E. de Mirandes, M. Cadoret, S. Guellati-Khelifa, C. Schwob, F. Nez, L. Julien, and F. Biraben, Precise measurement of h/m_{RB} using Bloch oscillations in a vertical optical lattice: Determination of the fine-structure constant, Phys. Rev. A **74**, 052109 (2006).

[27] R. Bouchendira, P. Cladé, S. Guellati-Khélifa, F. Nez, and F. Biraben, New Determination of the Fine Structure Constant and Test of the Quantum Electrodynamics, Phys. Rev. Lett. **106**, 080801 (2011).

[28] M. Kasevich and S. Chu, Atomic Interferometry Using Stimulated Raman Transitions, Phys. Rev. Lett. **67**, 181 (1991).

[29] E. Giese, A. Roura, G. Tackmann, E. M. Rasel, and W. P. Schleich, Double Bragg diffraction: A tool for atom optics, Phys. Rev. A **88**, 053608 (2013).

[30] H. Ahlers et al., Double Bragg Interferometry, Phys. Rev. Lett. **116**, 173601 (2016).

[31] J. Küber, F. Schmaltz, and G. Birkl, Experimental realization of double Bragg diffraction: robust beamsplitters, mirrors, and interferometers for Bose–Einstein condensates, arXiv:1603.08826.

[32] T. van Zoest et al., Bose–Einstein condensation in microgravity, Science **328**, 1540 (2010).

[33] J. Reichel, W. Hänsel, P. Hommelhoff, and T. W. Hänsch, Applications of integrated magnetic microtraps, Appl. Phys. B **72**, 81 (2001).

[34] J. M. McGuirk, G. T. Foster, J. B. Fixler, M. J. Snadden, and M. A. Kasevich, Sensitive absolute-gravity gradiometry using atom interferometry, Phys. Rev. A **65**, 033608 (2002).

[35] B. Cheng, P. Gillot, S. Merlet, and F. Pereira Dos Santos, Influence of chirping the Raman lasers in an atom gravimeter: Phase shifts due to the Raman light shift and to the finite speed of light, Phys. Rev. A **92**, 063617 (2015).

[36] P. Gillot, B. Cheng, S. Merlet, and F. Pereira Dos Santos, Limits to the symmetry of a Mach–Zehnder-type atom interferometer, Phys. Rev. A **93**, 013609 (2016).

[37] D. W. Allan, Statistics of atomic frequency standard, Proc. IEEE **54**, 221 (1966).

[38] P. Cheinet, B. Canuel, F. Pereira Dos Santos, A. Gauguet, F. Yver-Leduc, and A. Landragin, Measurement of the sensitivity function in a time-domain atomic interferometer, IEEE Trans. Instrum. Meas. **57**, 1141 (2008).

[39] A. Bonnin, N. Zahzam, Y. Bidel, and A. Bresson, Characterization of a simultaneous dual-species atom interferometer for a quantum test of the weak equivalence principle, Phys. Rev. A **92**, 023626 (2015).

[40] Other phase shifts are of minor relevance for our experimental parameters.

[41] German gravity network, http://www.bkg.bund.de/.

[42] F. Impens, P. Bouyer, and C. J. Bordé, Matter-wave cavity gravimeter, Appl. Phys. B **84**, 603 (2006).

[43] K. J. Hughes, J. H. T. Burke, and C. A. Sackett, Suspension of Atoms Using Optical Pulses, and Application to Gravimetry, Phys. Rev. Lett. **102**, 150403 (2009).

[44] J. M. McGuirk, M. J. Snadden, and M. A. Kasevich, Large Area Light-Pulse Atom Interferometry, Phys. Rev. Lett. **85**, 4498 (2000).

[45] T. Lévèque, A. Gauguet, F. Michaud, F. Pereira Dos Santos, and A. Landragin, Enhancing the Area of a Raman Atom Interferometer Using a Versatile Double-Diffraction Technique, Phys. Rev. Lett. **103**, 080405 (2009).

[46] H. Müller, S.-w. Chiow, Q. Long, S. Herrmann, and S. Chu, Atom Interferometry with up to 24-Photon-Momentum-Transfer Beam Splitters, Phys. Rev. Lett. **100**, 180405 (2008).

[47] S.-w. Chiow, T. Kovachy, H.-C. Chien, and M. A. Kasevich, $102\hbar k$ Large Area Atom Interferometers, Phys. Rev. Lett. **107**, 130403 (2011).

[48] T. Kovachy, S.-w. Chiow, and M. A. Kasevich, Adiabatic-rapid-passage multiphoton Bragg atom optics, Phys. Rev. A **86**, 011606 (2012).

[49] P. Cladé, S. Guellati-Khélifa, F. Nez, and F. Biraben, Large Momentum Beam Splitter Using Bloch Oscillations, Phys. Rev. Lett. **102**, 240402 (2009).

[50] H. Müller, S.-w. Chiow, S. Herrmann, and S. Chu, Atom Interferometers with Scalable Enclosed Area, Phys. Rev. Lett. **102**, 240403 (2009).

[51] G. D. McDonald, C. C. N. Kuhn, S. Bennetts, J. E. Debs, K. S. Hardman, M. Johnsson, J. D. Close, and N. P. Robins, $80\hbar k$ momentum separation with Bloch oscillations in an optically guided atom interferometer, Phys. Rev. A **88**, 053620 (2013).

[52] A. Sugarbaker, Ph.D. thesis, Stanford University, 2014.

[53] M. Andia, R. Jannin, F. Nez, F. Biraben, S. Guellati-Khélifa, and P. Cladé, Compact atomic gravimeter based on a pulsed and accelerated optical lattice, Phys. Rev. A **88**, 031605 (2013).

[54] R. Geiger et al., Detecting inertial effects with airborne matter-wave interferometry, Nat. Commun. **2**, 474 (2011).

[55] S. M. Dickerson, J. M. Hogan, A. Sugarbaker, D. M. S. Johnson, and M. A. Kasevich, Multiaxis Inertial Sensing with Long-Time Point Source Atom Interferometry, Phys. Rev. Lett. **111**, 083001 (2013).

[56] T. Kovachy, P. Asenbaum, C. Overstreet, C. A. Donnelly, S. M. Dickerson, A. Sugarbaker, J. M. Hogan, and M. A. Kasevich, Quantum superposition at the half-metre scale, Nature (London) **528**, 530 (2015).

[57] J. Rudolph et al., A high-flux BEC source for mobile atom interferometers, New J. Phys. **17**, 065001 (2015).

[58] G. Tackmann, P. Berg, C. Schubert, S. Abend, M. Gilowski, W. Ertmer, and E. M. Rasel, Self-alignment of a compact large-area atomic Sagnac interferometer, New J. Phys. **14**, 015002 (2012).

[59] V. Schkolnik, B. Leykauf, M. Hauth, C. Freier, and A. Peters, The effect of wavefront aberrations in atom interferometry, Appl. Phys. B **120**, 311 (2015).

[60] G. D'Agostino, S. Merlet, A. Landragin, and F. Pereira Dos Santos, Perturbations of the local gravity field due to mass distribution on precise measuring instruments: A numerical method applied to a cold atom gravimeter, Metrologia **48**, 299 (2011).

[61] A. Sugarbaker, S. M. Dickerson, J. M. Hogan, D. M. S. Johnson, and M. A. Kasevich, Enhanced Atom Interferometer Readout through the Application of Phase Shear, Phys. Rev. Lett. **111**, 113002 (2013).

[62] P. Zantye, A. Kumar, and A. Sikder, Chemical mechanical planarization for microelectronics applications, Mater. Sci. Eng. R **45**, 89 (2004).

[63] P. Böhi, M. F. Riedel, J. Hoffrogge, J. Reichel, T. W. Hänsch, and P. Treutlein, Coherent manipulation of Bose–Einstein condensates with state-dependent microwave potentials on an atom chip, Nat. Phys. **5**, 592 (2009).

[64] H.-C. Chuang, C.-W. Weng, and H.-F. Li, Design, microfabrication and characterization of planarized multilayer atom chips with enhanced heat dissipation, J. Micromech. Microeng. **21**, 125009 (2011).

[65] E. Giese, A. Friedrich, S. Abend, E. M. Rasel, and W. P. Schleich, Light shifts in atomic Bragg diffraction, Phys. Rev. A (to be published).

[66] P. Hamilton, M. Jaffe, J. M. Brown, L. Maisenbacher, B. Estey, and H. Müller, Atom Interferometry in an Optical Cavity, Phys. Rev. Lett. **114**, 100405 (2015).